8902 *Biochemistry* **2010,** *49,* 8902–8911
DOI: 10.1021/bi1008672

BIOCHEMISTRY
including biophysical chemistry & molecular biology
Article

Global Fit Analysis of Glucose Binding Curves Reveals a Minimal Model for Kinetic Cooperativity in Human Glucokinase[†]

Mioara Larion and Brian G. Miller*

Department of Chemistry and Biochemistry, The Florida State University, Tallahassee, Florida 32306-4390

Received May 28, 2010; Revised Manuscript Received August 18, 2010

ABSTRACT: Human pancreatic glucokinase is a monomeric enzyme that displays kinetic cooperativity, a feature that facilitates enzyme-mediated regulation of blood glucose levels in the body. Two theoretical models have been proposed to describe the non-Michaelis−Menten behavior of human glucokinase. The mnemonic mechanism postulates the existence of one thermodynamically favored enzyme conformation in the absence of glucose, whereas the ligand-induced slow transition model (LIST) requires a preexisting equilibrium between two enzyme species that interconvert with a rate constant slower than turnover. To investigate whether either of these mechanisms is sufficient to describe glucokinase cooperativity, a transient-state kinetic analysis of glucose binding to the enzyme was undertaken. A complex, time-dependent change in enzyme intrinsic fluorescence was observed upon exposure to glucose, which is best described by an analytical solution comprised of the sum of four exponential terms. Transient-state glucose binding experiments conducted in the presence of increasing glycerol concentrations demonstrate that three of the observed rate constants decrease with increasing viscosity. Global fit analyses of experimental glucose binding curves are consistent with a kinetic model that is an extension of the LIST mechanism with a total of four glucose-bound binary complexes. The kinetic model presented herein suggests that glucokinase samples multiple conformations in the absence of ligand and that this conformational heterogeneity persists even after the enzyme associates with glucose.

Glucokinase (HK-IV, hexokinase D) catalyzes the ATP-dependent phosphorylation of glucose in the first step of glycolysis, a transformation that represents the rate-limiting reaction of glucose metabolism in the liver and pancreas (*1*−*3*). Heterozygous inactivating mutations in the glucokinase gene cause maturity onset diabetes of the young 2 (MODY2),[1] whereas homozygous inactivating lesions produce a more severe condition known as permanent neonatal diabetes mellitus (PNDM) (*4*, *5*). Under steady-state conditions, glucokinase activity displays a sigmoidal response to increasing glucose concentrations that is characterized by a Hill equation with a coefficient of 1.7. While kinetic cooperativity is observed with respect to glucose, traditional Michaelis−Menten kinetics are observed when the concentration of the second substrate, $MgATP^{2-}$, is varied in the presence of saturating glucose levels (*6*). The existence of kinetic cooperativity in human glucokinase is intriguing because the enzyme functions exclusively as a monomer under physiological conditions (*7*, *8*). Although a number of mechanisms for kinetic cooperativity in monomeric enzymes have been proposed in the literature, the mnemonic and the ligand-induced slow transition (LIST) models have received the most attention in recent studies of glucokinase (*9*−*14*).

Ricard, Meunier, and Buc first formulated the mnemonic model for cooperativity in monomeric enzymes in 1974 (*13*, *15*−*17*). It was based upon earlier conceptual work by Rabin and Frieden, who postulated that the conformation of an enzyme following product release could be different from the initial state (*18*, *19*). The mnemonic model postulates that an enzyme is capable of oscillating between two conformationally distinct species, a low-affinity state (E′) and a high-affinity state (E) (Figure 1A). According to the mnemonic mechanism, only the low-affinity conformation exists in the absence of substrate. The catalytic cycle begins when glucose binds to the low-affinity state and induces a conformational change to the high-affinity state. This conformational transition is slow, presumably because the conversion involves significant structural rearrangements. Upon reaching the high-affinity state, glucokinase rapidly binds ATP to generate the ternary complex, where catalysis occurs. Release of products ADP and glucose 6-phosphate is permitted from the high-affinity state. If substrate glucose is abundant, the high-affinity state can rapidly undergo a second round of catalysis without formation of the slowly realized, low-affinity conformation. If glucose concentrations are low, however, sufficient time exists for the enzyme to relax to the low-affinity conformation before another molecule of glucose binds. According to the mnemonic model, this slow relaxation step prevents conformational equilibration from being reached during the catalytic cycle, a condition that results in cooperativity.

The ligand-induced slow transition (LIST) model developed by Neet and co-workers provides a more general mechanism for explaining kinetic cooperativity in monomeric enzymes (*14*, *20*−*23*).

[†]This work was supported, in part, by grants from the James and Ester King Biomedical Research Program (09KN08) and from the National Institute of Diabetes and Digestive and Kidney Diseases (DK081358).

*To whom correspondence should be addressed: 217 Dittmer Laboratory of Chemistry, Department of Chemistry and Biochemistry, The Florida State University, Tallahassee, FL 32306-4390. Telephone: (850) 645-6570. Fax: (850) 644-8281. E-mail: miller@chem.fsu.edu.

[1]Abbreviations: GK, glucokinase; OD, optical density; TCEP, tris(2-carboxyethyl)phosphine; LIST, ligand-induced slow transition model; HEPES, 4-(2-hydroxyethyl)-1-piperazineethanesulfonic acid; MODY2, maturity onset diabetes of the young 2; HI, hyperinsulinemia of infancy.

 Published on Web 09/09/2010

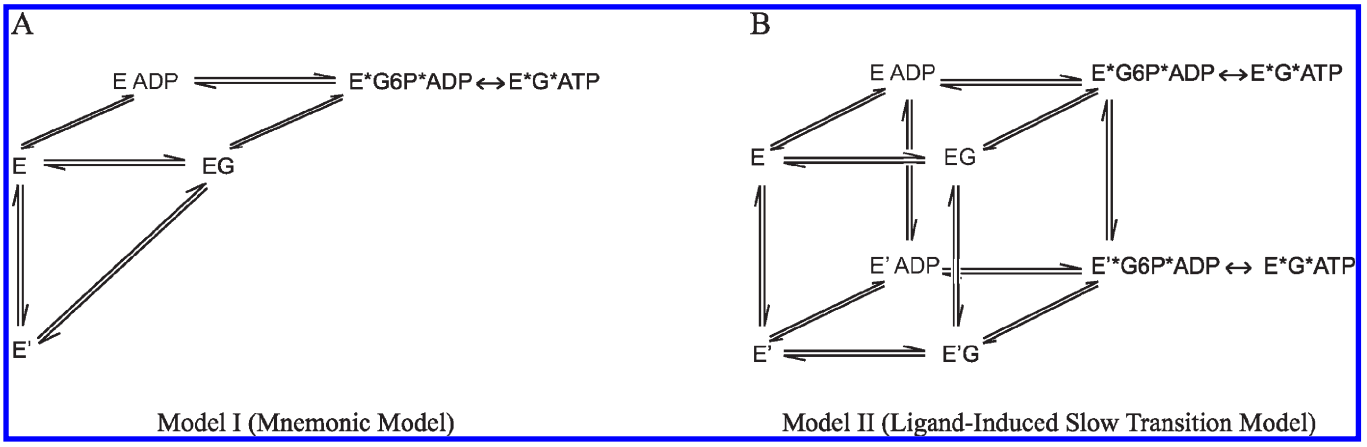

FIGURE 1: Two previously proposed kinetic models for cooperativity in monomeric human glucokinase. The mnemonic model (A) postulates the existence of a single thermodynamic favored state in the absence of ligand, E′, whereas the ligand-induced slow transition (LIST) model (B) postulates the existence of two catalytic cycles involving two conformationally distinct species. In both models, the rate of interconversion of E and E′ is slower than k_{cat}.

Similar to the mnemonic model, the LIST mechanism involves the existence of two distinct enzyme conformations, E and E′. In the LIST model, however, the enzyme is characterized by a preexisting equilibrium that involves two conformationally distinct species in the absence of substrate (Figure 1B). These two conformations possess different affinities for substrate glucose, and the equilibrium between these states is controlled by the concentration of glucose. Similar to the mnemonic model, the LIST mechanism requires that the conformational equilibration between enzyme states be slower than catalysis. In the LIST mechanism, two separate catalytic cycles are possible, whereas the mnemonic model requires only one catalytically active enzyme species. According to the LIST model, the steady-state velocity of the glucokinase reaction is the sum of the rates of the two cycles.

Support for both the mnemonic and LIST mechanisms can be found within experimental data collected on glucokinase over the past 40 years (*20*−*29*). For example, the observation of decreased glucose cooperativity at limiting $MgATP^{2-}$ concentrations, or when a poorly reacting nucleotide replaced $MgATP^{2-}$, was thought to support the mnemonic model prediction that cooperativity depends upon the ability of the second substrate to react rapidly with the binary enzyme−glucose complex (*25*). More recently, Kamata and co-workers succeeded in determining the three-dimensional structure of human pancreatic glucokinase both in the unliganded state and in the presence of glucose and a synthetic small molecule activator (*30*). The ability of these investigators to isolate and structurally characterize a single unliganded enzyme species was interpreted in terms of the mnemonic model. Evidence in support of the LIST mechanism includes the observation of a Hill coefficient of < 1 at low $MgATP^{2-}$ concentrations, a condition that requires more than one catalytic cycle (*22*).

In recent years, a number of transient-state kinetic investigations of the binding of glucose to the human enzyme have also produced conflicting reports regarding the mechanism of glucokinase cooperativity. The first of these studies was conducted by Heredia and co-workers, who reported a biphasic response of glucokinase intrinsic fluorescence upon glucose association (*31*). The resulting kinetic data fit best to a reversible two-step mechanism, which was consistent with the mnemonic model. In a subsequent study, Kim et al. reported that the intrinsic fluorescence of the enzyme displayed a monophasic response to glucose association, although the associated k_{obs} exhibited a biphasic dependence upon glucose concentration (*32*). These authors interpreted their data in terms of the LIST model, in which the preexisting equilibrium involves a high-affinity species that displays a glucose K_d value of 90 μM, while the low-affinity state is characterized by a glucose K_d value of 73 mM. The most recent report about glucose binding using transient-state kinetic methods was published by Antoine and colleagues, who found that glucose binding traces take a long period of time to reach equilibrium (> 100 s) and are best described by a sum of four exponential terms (*33*). The phase with the highest amplitude, k_{obs3}, exhibited the same biphasic behavior as the observed rate constant previously described by Kim. Antoine simulated the dependence of k_{obs3} upon increasing glucose concentrations and used these results to predict the existence of at least two unliganded conformations with different glucose affinities and two slowly interconverting binary enzyme−glucose complexes.

In this study, we report the results of our own investigations of the transient-state kinetic behavior of human pancreatic glucokinase. In contrast to the aforementioned studies, we employed high enzyme concentrations and conducted viscosity and temperature variation studies to investigate glucose binding kinetics. Our experimental glucose binding curves were fit to a variety of mechanistically distinct models using numerical integration of the relevant rate equations. The results of these global fit analyses provided a poor fit to previously proposed models, including simplified versions of both the mnemonic and ligand-induced slow transition (LIST) mechanisms. On the other hand, our kinetic data require a minimal kinetic mechanism that includes two conformationally distinct ligand free species and four structurally unique binary enzyme−glucose complexes. Our global fit analysis also provides an estimate for individual microscopic rate constants describing the glucose binding process, data that afford useful benchmarks for future experimental investigations of glucokinase kinetic cooperativity.

MATERIALS AND METHODS

Protein Expression and Purification. Recombinant human pancreatic glucokinase was produced as an N-terminal hexahistidine-tagged polypeptide in glucokinase-deficient *Escherichia coli* strain BM5340(DE3). Bacterial cultures were inoculated to an initial OD_{600} of 0.01 and were grown at 37 °C in Luria-Bertani broth supplemented with ampicillin (150 μg/mL), kanamycin (40 μg/mL), and chloramphenicol (25 μg/mL). When the OD_{600} reached 0.85, IPTG (1 mM) was added to induce gene expression

and the temperature was reduced to 20 °C, where growth was continued for 20 h. Cells were harvested by centrifugation at 8000*g*, and 5 g of wet cell pellet was resuspended in 17 mL of buffer A containing HEPES (50 mM, pH 7.6), KCl (50 mM), imidazole (40 mM), dithiothreitol (10 mM), and glycerol (25%, w/v). Cells were lysed using a French press and subjected to centrifugation at 25000*g* and 4 °C for 1 h. The supernatant was immediately loaded onto a 5 mL HisTrap Fast Flow Affinity Column (GE Healthcare) previously equilibrated in buffer A. Following loading, the column was washed with 10 column volumes of buffer A followed by 5 columns of buffer A containing 65 mM imidazole. Glucokinase was eluted with buffer A containing 250 mM imidazole, and the enzyme was dialyzed overnight at 4 °C against 1 L of buffer containing HEPES (50 mM, pH 7.6), KCl (50 mM), and dithiothreitol (10 mM). To validate the performance of our enzyme in transient-state kinetic experiments, we purified a sample of recombinant human glucokinase using an additional size-exclusion chromatography step following affinity column purification. For these experiments, dialyzed glucokinase was injected onto a Superose 6 10/300 gel filtration column (Amersham-Pharmacia) pre-equilibrated in a buffer containing HEPES (50 mM, pH 7.6), KCl (50 mM), and dithiothreitol (10 mM). The gel filtration column was run at a flow rate of 0.02 mL/min, and fractions containing the highest A_{280} readings were pooled and retained for further analysis. We detected no difference in the transient-state kinetic data when the size-exclusion chromatography step was included. Thus, to maximize the enzyme concentration and the signal-to-noise ratio of transient fluorescence data, affinity column-purified recombinant glucokinase that was judged to be >95% pure on the basis of sodium dodecyl sulfate−polyacrylamide gel electrophoresis (SDS−PAGE) analysis was used in transient-state binding experiments. The presence of a 5% impurity in the enzyme preparation is not expected to significantly impact the measured changes in fluorescence that accompany the binding of glucose to glucokinase.

Equilibrium Binding and Transient-State Kinetic Experiments. For equilibrium glucose binding studies, proteins were purified as described above and were dialyzed against HEPES (50 mM, pH 7.6), NaCl (50 mM), DTT (10 mM), and glycerol (5%, w/v) prior to data collection. Binding affinities were determined by monitoring the change in fluorescence at 335 nm that occurred in the presence of varying glucose concentrations (0.010−100 mM) following excitation of glucokinase (10 μM) at 280 nm using a 5 nm slit width, as previously described (*34*). Briefly, enzyme and glucose were mixed in 0.5 mL, 1.0 cm path length cuvettes in a buffer containing sodium phosphate (5 mM, pH 7.6), KCl (25 mM), and DTT (10 mM). Equilibrium binding experiments were performed on a Cary Eclipse fluorescence spectrometer housed in the Physical Biochemistry Laboratory in the Institute for Molecular Biophysics. Data were collected in duplicate, averaged, and fitted to the following equation:

$$\Delta F = \frac{\Delta F_{\max}[\text{glucose}]}{K_m + [\text{glucose}]}$$

Transient-state binding data were collected on an Applied Photophysics SX20 stopped-flow spectrometer housed in the Protein Biophysics Laboratory in the Institute for Molecular Biophysics at The Florida State University. Sample syringes were maintained at the appropriate temperature with a circulating water bath. Glucokinase was excited at 280 nm, and the emission spectrum was monitored using a 320 nm cutoff filter. At least five transient fluorescence traces were obtained at each glucose concentration, and the multiple traces were averaged prior to analysis using the curve fitting program of the instrument. Fluorescence traces were collected for a total of 250 s using a log scale to obtain the fast phase kinetics. At time frames above 250 s, a decrease in the magnitude of the protein fluorescence signal was observed, presumably because of photobleaching of the sample. A variety of enzyme concentrations (1−39 μM) were investigated to maximize the fluorescence signal. To verify the existence of multiple exponential terms in the binding traces, several control experiments were conducted. Enzyme was pre-incubated with glucose and mixed with buffer in the stopped-flow instrument to measure the dissociation rates. These experiments showed the same number of exponential terms as the binding experiments, indicating that the number of transitions observed during glucose binding was authentic. The hexahistidine tag was removed via insertion of a specific seven-amino acid sequence (Glu-Asn-Leu-Phe-Tyr-Gln-Ser), followed by cleavage between Gln and Ser with TEV protease. Transient-state glucose binding curves using the cleaved enzyme showed the same number of exponential terms as the His-tagged version of the protein.

Technical optimizations were needed to eliminate a random artifact signal observed when the enzyme was initially mixed with buffer, the amplitude of which was significant enough to interfere with the amplitude of the fastest transient observed. These optimizations included increasing the number of drives between acquisitions from one to four, decreasing the slit width (from 2 to 0.165 nm), decreasing the mixing pressure (from 60 to 20 psi), and increasing the incubation time at the appropriate temperature prior to acquisition (from 5 to 40 min). The observed artifact appeared to be associated with the mixing pressure. Indeed, exposing the enzyme to high pressures (60 psi) such as those routinely used to mix reagents in the stopped-flow loop caused an 80% loss of the enzymatic activity of human glucokinase. A maximum mixing pressure of 30 psi allowed the preservation of the full enzymatic activity. Because the traces were recorded on the order of minutes, photobleaching was initially observed as a decrease in the magnitude of the fluorescence signal. To eliminate this effect, we decreased the slit width (0.165 nm) until a straight baseline was observed up to 250 s after mixing enzyme and buffer. The kinetic rate constants and amplitudes as a function of ligand concentration were determined from the time-dependent change in fluorescence intensity by fitting the binding curves to a quadruple-exponential equation of the form

$$I(t) = \sum_{i=1}^{n} (A_i e^{-k_{\text{obs}i}t}) + C$$

where $I(t)$ is the intensity of the fluorescence signal at time t, n is the number of exponentials, A_i is the amplitude of the ith exponential, $k_{\text{obs}i}$ is the observed rate constant for the ith exponential, and C is a constant corresponding to the asymptotic signal limit.

Pre-Equilibrium Viscosity and Temperature Variation Experiments. To assess the degree to which viscosity affected the number and rates of the observed transients, different glycerol concentrations were added to the stopped-flow buffers. Addition of glycerol caused alterations in the k_{obs} values associated with glucose binding, without affecting the overall number of exponential terms needed to fit the data. Solutions containing 5, 10,

20, and 40% glycerol (w/v) were used to equilibrate the enzyme and to prepare 2× stock solutions of the appropriate glucose concentration. Relative viscosities of glycerol solutions were measured using a Cannon-Fenske viscometer. For temperature variation experiments, the temperature was set to either 25 or 10 °C on the water bath unit of the Applied Photophysics SX20 stopped-flow spectrometer, and samples from ice were allowed to equilibrate for at least 10 min prior to data acquisition.

Global Fit Analysis of Glucose Binding Curves. The transient-state kinetics of glucose binding and dissociation were best described by an analytical solution comprised of the sum of four exponential terms. To gain insight into the significance of the observed rate constants, we attempted to fit the experimental traces to different kinetic models. Glucose binding traces were averaged, normalized, and imported into Pro-Kineticist II from Applied Photophysics (*35*). To fit the family of glucose binding curves, fluorescence data were normalized by dividing the signal by the initial fluorescence intensity. The initial fluorescence intensity is constant because the same concentration of enzyme was used in each binding experiment. The normalization was performed to avoid fluctuations in the signal due to changes in the detector's voltage between acquisitions. Pro-Kineticist II allows the simultaneous fitting of glucose binding curves to a unique kinetic mechanism via numerical integration. Data collected during the first 5 ms were eliminated from each binding trace prior to fitting. Glucose concentrations used in the experiment (3−96 mM) were introduced as initial parameters in the program along with estimated concentration values for individual enzyme species. Initially, we considered a simplified kinetic model containing only a single enzyme conformation in the absence of ligand. Other mechanistic variations that were considered included the glucose binding component of the LIST and mnemonic models, as well as models that included more than two enzyme conformations. Initial values for individual microscopic rate constants were chosen arbitrarily, and each parameter was allowed to vary until the optimal sum of squares value was obtained. At this stage, a visual inspection of the observed microscopic rate constants was performed to identify reasonable rate constants with low error values. These values were fixed, while the remaining rate constants were refined in a second simulation step to produce a completed fit. For kinetic models that involved more than one enzyme conformation, different concentrations of E and E′ were investigated.

We investigated the extent to which the values of the fitted microscopic rate constants were constrained by our experimental data within the context of the final kinetic model. To do so, we fixed individual rate constants, one at a time, to values that were either 10-fold higher or 10-fold lower than the best fit value. The 13 remaining rate constants were permitted to vary, and the simulation was allowed to proceed through a single iteration. If the resulting sum of squares value changed by more than 10-fold as compared to the best fit sum of squares (SSQ) value, the microscopic rate constant was considered constrained. The different kinetic models investigated by global fit analysis were not nested and contained a differing number of parameters. Thus, we applied Akaike's Information Criterion (AIC) to compare the relative significance of the increased goodness of fit, as reflected in the SSQ value, with increasing numbers of fitting parameters (*36*):

$$\mathrm{AIC} = N \times \ln\left(\frac{\mathrm{SSQ}}{N}\right) + 2K$$

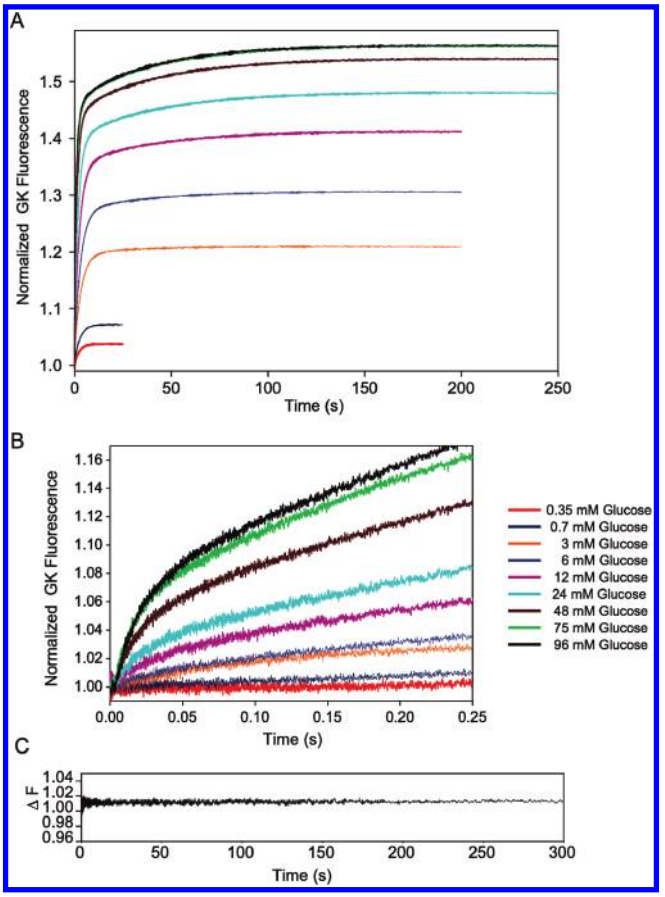

FIGURE 2: (A) Pre-equilibrium kinetics of binding of glucose (0.35−96 mM) to human pancreatic glucokinase (39 μM). (B) Pre-equilibrium burst observed within 50 ms of the enzyme and glucose being mixed. (C) The fluorescence signal of enzyme alone is unchanged during the time course of observation, demonstrating negligible photobleaching of the sample.

where N is the number of data points, SSQ is the sum of squares values for each model, and K represents the number of parameters fitted by Pro-Kineticist II. The model with the lowest AIC value is considered the "best" model based upon the SSQ values and the balance between the change in the goodness of fit and the change in the number of parameters to be fitted. Applying the AIC method resulted in the following rank order of models, from best to worst: model VI, model V, model II, model IV, model I, and model III (Table S2 of the Supporting Information).

RESULTS

Equilibrium Binding of Glucose to Human Pancreatic Glucokinase. Equilibrium binding of glucose to glucokinase was monitored by measuring the change in the enzyme's intrinsic fluorescence at increasing concentrations of glucose. Consistent with earlier reports, cooperativity was not observed in our equilibrium measurements. The dissociation constant for glucose determined from these experiments was 5 mM. Interestingly, this thermodynamic constant is not significantly different from the glucose $K_{0.5}$ value (8.1 mM) determined from steady-state kinetic assays. On the basis of our experimentally determined glucose K_d value, we chose to conduct transient-state binding experiments over a glucose concentration range of 0.35−96 mM.

Transient-State Binding of Glucose to Glucokinase. Transient-state binding experiments were conducted by mixing a range of glucose concentrations with high concentrations of the recombinant enzyme using a stopped-flow spectrometer. Binding

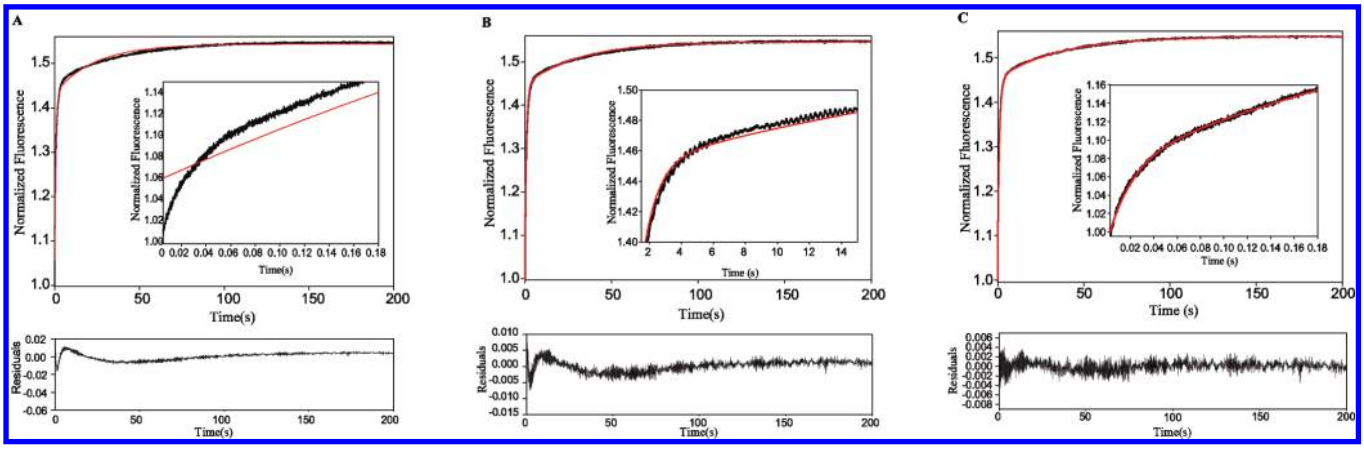

FIGURE 3: Glucose binding curves require an analytical solution comprised of the sum of four exponential terms for glucose concentrations of >3 mM. Attempts to fit the 96 mM glucose binding curve (black) to an analytical solution (red) comprised of the sum of two exponential terms (A), three exponential terms (B), and four exponential terms (C). The quality of the fit in the fast regime is shown in the inset, and the residuals associated with each fit are shown below the binding curves.

curves were obtained at nine different glucose concentrations and were collected over times ranging from 5 ms to 250 s (Figure 2). The resulting traces were fit to a variety of exponential functions in an attempt to arrive at an analytical solution that best described each curve. At glucose concentrations of <1 mM, an analytical solution consisting of the sum of two exponential terms was sufficient to describe the binding curves. The addition of a third exponential term to the analytical solution was necessary to accurately represent binding transients at glucose concentrations between 1 and 3 mM. At higher glucose concentrations, however, a triple-exponential function correlated poorly with the experimental data in both the fast and intermediate time regimes. Thus, a fourth exponential term was required to fit glucose binding curves at glucose concentrations of >3 mM (Figure 3A−C). Because of the differential number of observable events detected at low glucose concentrations, we considered only binding curves for glucose concentrations of ≥3 mM in our subsequent global fit analyses. Transient-state dissociation kinetics conducted at high glucose concentrations confirmed the existence of four kinetically distinguishable events (Figure S1 of the Supporting Information). Similarly, four exponential terms were required to accurately fit binding curves obtained at saturating concentrations of the noncooperative substrate 2-deoxyglucose (Figure S2 of the Supporting Information).

The observed amplitudes and rate constants of the four kinetically distinguishable events detected in our transient-state experiments displayed a complex behavior as a function of increasing glucose concentrations (Figures 4 and 5). The two fastest observable rate constants, k_{obs1} and k_{obs2}, appear to display hyperbolic dependencies on glucose concentration. The value of k_{obs2} appears to be more steeply dependent upon glucose concentration, reaching a maximum value near 10 mM, whereas the value of k_{obs1} does not reach a maximum until 50 mM glucose. The normalized amplitudes of both k_{obs1} and k_{obs2} increase linearly as a function of increasing glucose concentration. The third observable rate constant, k_{obs3}, appears to display a sigmoidal dependence upon glucose concentration. The amplitude of k_{obs3} increases sharply with increasing glucose concentrations up to 24 mM, and then it decreases as glucose levels are increased to 96 mM. The value of the slowest rate constant, k_{obs4}, initially decreases with increasing glucose concentrations up to 24 mM. A slight increase in the value of this rate constant can be observed at glucose concentrations between 24 and 96 mM. The amplitude of k_{obs4} displays a hyperbolic dependence upon glucose concentration.

Effects of Viscosity and Temperature on Glucose Binding. To provide insight into the physical basis of the four kinetically distinguishable events observed in our transient-state glucose binding curves, we altered both the viscosity and temperature at which binding occurred. Increasing the relative viscosity of the solution via the addition of glycerol caused a decrease in the values of k_{obs1}, k_{obs2}, and k_{obs3} without altering the number of exponential terms required in the analytical solution used to fit each binding curve (Table 1). In contrast, the value of k_{obs4} was largely unaffected by the increase in solution viscosity. At 3 mM glucose (the lowest concentration analyzed), there was a high degree of variability in the values of several rate constants, a fact that may be attributable to the low amplitude of this signal at diminishing glucose concentrations.

In an attempt to obtain a better separation of the individual signals observed during glucose binding, we decreased the temperature to 10 °C. Under these conditions, the analytical solution that provided the best fit to the experimental data requires three or fewer exponential terms at glucose concentrations of <12 mM. At glucose concentrations above this value, the decreased temperature produced lower values for k_{obs1} and k_{obs3}, while having only modest effects upon k_{obs2} and k_{obs4} (Table 2).

Global Fit Analyses of Transient Glucose Binding Kinetics. Pro-Kineticist II from Applied Photophysics was used to fit the glucose binding data collected at 25 °C, in the absence of added glycerol, to a variety of mechanistic postulates (*35*). Pro-Kineticist II enables one to perform a global fit analysis of kinetic data obtained under a variety of experimental concentrations to a user-specified model. The resulting fit provides an assessment of how well the experimental data can be fit to a given kinetic model, as reflected in the sum of squares value. The fit also provides an estimate of the microscopic rate constants for individual events described in the specified model. In this study, we investigated a variety of kinetic pathways for binding of glucose to human glucokinase, two of which are shown in Figure 1 and four of which are depicted in Figure 6. Binding curves obtained at glucose concentrations of <3 mM were not included in the global fit analyses because of their failure to require four exponential terms for their accurate description. Presumably, this is due to an inability to detect certain binding processes at dilute substrate concentrations.

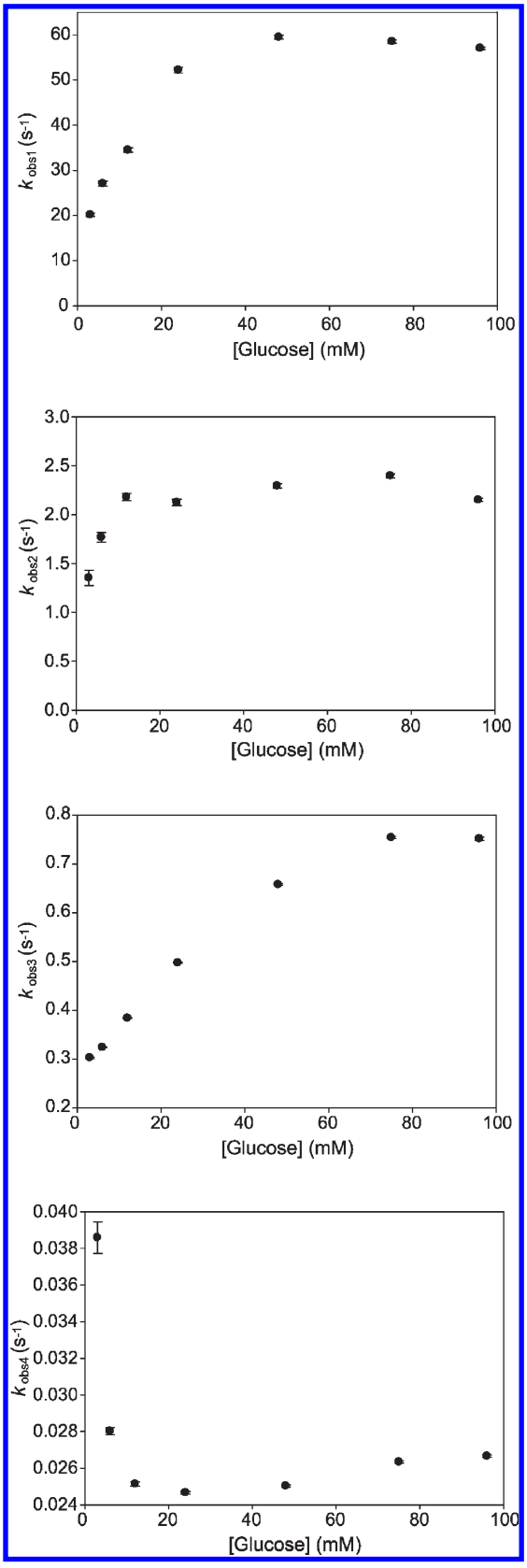

FIGURE 4: Magnitude of the four observed rate constants as a function of glucose concentrations. The k_{obs} values were obtained by fitting the data to an analytical solution comprised of four exponential terms. Error bars represent the goodness of fit between the experimental data and the analytical solution.

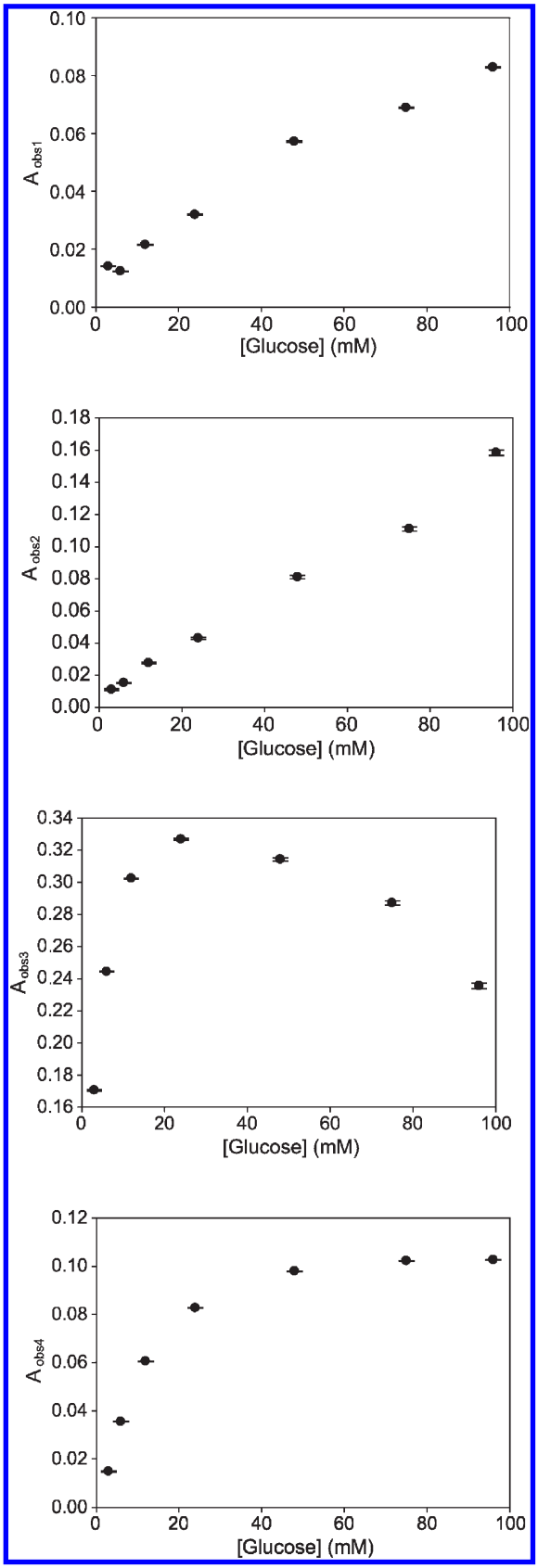

FIGURE 5: Amplitudes of the four observed transient signals as a function of glucose concentration. The amplitudes were obtained by fitting the data to an analytical solution comprised of four exponential terms. Error bars represent the goodness of fit between the experimental data and the analytical solution.

The glucose binding component of the mnemonic model [model I (Figure 1A)] and the LIST mechanism [model II (Figure 1B)] failed to provide a good fit to our experimental data, as judged by their respective sum of squares values, 49 and

Table 1: Observed Rate Constants Associated with Glucose Binding at Different Viscosities

[glucose] (mM)	% glycerol (w/v) (relative viscosity)	k_{obs1}	k_{obs2}	k_{obs3}	k_{obs4}
96	0 (1.0)	57 ± 0.3	2.2 ± 0.02	0.75 ± 0.003	0.027 ± 0.0001
	5 (1.2)	44 ± 0.2	2.2 ± 0.01	0.77 ± 0.002	0.029 ± 0.0001
	10 (1.4)	43 ± 0.2	2.1 ± 0.01	0.70 ± 0.002	0.028 ± 0.0001
	20 (1.9)	35 ± 0.2	1.5 ± 0.01	0.54 ± 0.003	0.025 ± 0.0001
	40 (4.3)	16 ± 0.1	0.9 ± 0.01	0.20 ± 0.001	0.022 ± 0.0001
75	0 (1.0)	58 ± 0.4	2.4 ± 0.02	0.75 ± 0.002	0.026 ± 0.0001
	5 (1.2)	59 ± 0.3	2.6 ± 0.02	0.76 ± 0.002	0.028 ± 0.0001
	10 (1.4)	43 ± 0.2	2.2 ± 0.01	0.66 ± 0.001	0.026 ± 0.0001
	20 (1.9)	27 ± 0.2	1.5 ± 0.01	0.51 ± 0.001	0.024 ± 0.0001
	40 (4.3)	17 ± 0.2	0.9 ± 0.01	0.25 ± 0.001	0.020 ± 0.0001
48	0 (1.0)	59 ± 0.5	2.3 ± 0.02	0.66 ± 0.002	0.025 ± 0.0001
	5 (1.2)	38 ± 0.2	2.1 ± 0.02	0.62 ± 0.001	0.028 ± 0.0001
	10 (1.4)	35 ± 0.2	2.1 ± 0.01	0.56 ± 0.001	0.026 ± 0.0001
	20 (1.9)	27 ± 0.3	1.5 ± 0.02	0.44 ± 0.001	0.022 ± 0.0001
	40 (4.3)	17 ± 0.3	0.9 ± 0.02	0.22 ± 0.001	0.019 ± 0.0001
24	0 (1.0)	52 ± 0.7	2.1 ± 0.03	0.49 ± 0.001	0.025 ± 0.0001
	5 (1.2)	42 ± 0.3	2.5 ± 0.03	0.47 ± 0.001	0.027 ± 0.0001
	10 (1.4)	48 ± 0.3	2.4 ± 0.02	0.39 ± 0.001	0.025 ± 0.0001
	20 (1.9)	15 ± 0.2	1.2 ± 0.02	0.29 ± 0.001	0.022 ± 0.0001
	40 (4.3)	19 ± 0.2	0.9 ± 0.01	0.14 ± 0.001	0.018 ± 0.0001
12	0 (1.0)	34 ± 0.5	2.2 ± 0.04	0.38 ± 0.001	0.025 ± 0.0001
	5 (1.2)	45 ± 0.6	2.7 ± 0.03	0.35 ± 0.001	0.028 ± 0.0001
	10 (1.4)	36 ± 0.5	2.4 ± 0.02	0.27 ± 0.001	0.026 ± 0.0001
	20 (1.9)	7.0 ± 0.3	1.2 ± 0.05	0.18 ± 0.001	0.021 ± 0.0001
	40 (4.3)	9.0 ± 0.2	0.6 ± 0.01	0.09 ± 0.001	0.017 ± 0.0001
6	0 (1.0)	27 ± 0.5	1.8 ± 0.05	0.32 ± 0.001	0.028 ± 0.0002
	5 (1.2)	20 ± 0.3	1.6 ± 0.05	0.28 ± 0.001	0.031 ± 0.0002
	10 (1.4)	16 ± 0.3	1.6 ± 0.03	0.21 ± 0.001	0.028 ± 0.0001
	20 (1.9)	16 ± 0.4	1.3 ± 0.03	0.14 ± 0.001	0.024 ± 0.0001
	40 (4.3)	14 ± 0.7	0.8 ± 0.02	0.06 ± 0.001	0.015 ± 0.0001
3	0 (1.00)	20 ± 0.4	1.4 ± 0.08	0.30 ± 0.001	0.039 ± 0.001
	5 (1.2)	22 ± 0.6	1.5 ± 0.08	0.26 ± 0.001	0.046 ± 0.001
	10 (1.4)	3.0 ± 0.3	0.7 ± 0.34	0.18 ± 0.002	0.051 ± 0.001
	20 (1.9)	19 ± 0.8	1.0 ± 0.04	0.11 ± 0.001	0.035 ± 0.001
	40 (4.3)	18 ± 0.3	0.6 ± 0.014	0.05 ± 0.001	0.015 ± 0.0001

Table 2: Temperature Dependence of the Observed Rate Constants[a]

[glucose] (mM)	temp (°C)	k_{obs1}	k_{obs2}	k_{obs3}	k_{obs4}
96	25	57 ± 0.3	2.2 ± 0.1	0.75 ± 0.003	0.027 ± 0.001
	10	20 ± 3.4	2.2 ± 0.5	0.20 ± 0.003	0.015 ± 0.001
75	25	59 ± 0.4	2.4 ± 0.1	0.75 ± 0.002	0.026 ± 0.001
	10	22 ± 3.6	2.8 ± 0.5	0.20 ± 0.002	0.017 ± 0.002
48	25	59 ± 0.5	2.3 ± 0.1	0.66 ± 0.002	0.025 ± 0.001
	10	20 ± 2.9	2.7 ± 0.7	0.17 ± 0.002	0.021 ± 0.003
24	25	52 ± 0.6	2.1 ± 0.1	0.49 ± 0.001	0.025 ± 0.001
	10	24 ± 2.6	2.7 ± 0.4	0.14 ± 0.003	0.048 ± 0.009
12	25	34 ± 0.5	2.2 ± 0.1	0.38 ± 0.001	0.025 ± 0.001
	10	22 ± 0.9	3.7 ± 1.1	0.47 ± 0.17	0.102 ± 0.015

[a]Traces collected at < 12 mM glucose and 10 °C were not included because of their failure to be fitted to a four-exponential function.

3.1. Next, we explored whether the inclusion of additional unliganded enzyme species or additional binary enzyme−glucose complexes improved the fit. The sum of squares value obtained for model III (Figure 6A), which includes three distinct enzyme−glucose complexes, was 690. The sum of squares values for models IV and V (Figure 6B,C), which contain multiple ligand free species and multiple interconverting glucose-bound states, were 5.1 and 1.7, respectively. Kinetic model VI (Figure 6D) produced the best fit to our experimental glucose binding data and yielded a sum of squares value of < 1. A comparison of the fit to the experimental data for each model tested is available as Supporting Information (Figures S3−S8). Statistical analysis employing the AIC method demonstrated that model VI provides a statistically significant improvement in the goodness of fit when compared to other models with fewer fitting parameters (Table S1 of the Supporting Information).

The global fit analysis for model VI also provided an estimate for the values of the microscopic rate constants, which are detailed in Table 3. To evaluate whether the fitted values of the microscopic rate constants are constrained well by our experimental data, error analysis was performed. We investigated the reliability of both the upper and lower limits for each rate constant value by exploring the sensitivity of the sum of squares value to variations in individual rate constants, as described in Materials and Methods. These studies demonstrate that several of the microscopic rate constants are underrepresented by the glucose binding traces. For example, the upper limits of k_1, k_6, and k_7 are poorly constrained, as are the lower limits for the values of k_{-1}, k_{-2}, k_{-6}, and k_{-7}. The values of k_2 are poorly constrained in both directions. Rate constants that were judged to be ill-defined in any direction are denoted with an asterisk in Table 3. We also derived an expression for the apparent glucose K_d value in terms of the microscopic rate constants reflected in model VI and obtained reasonable agreement between the experimental and calculated dissociation constants (Supporting Information).

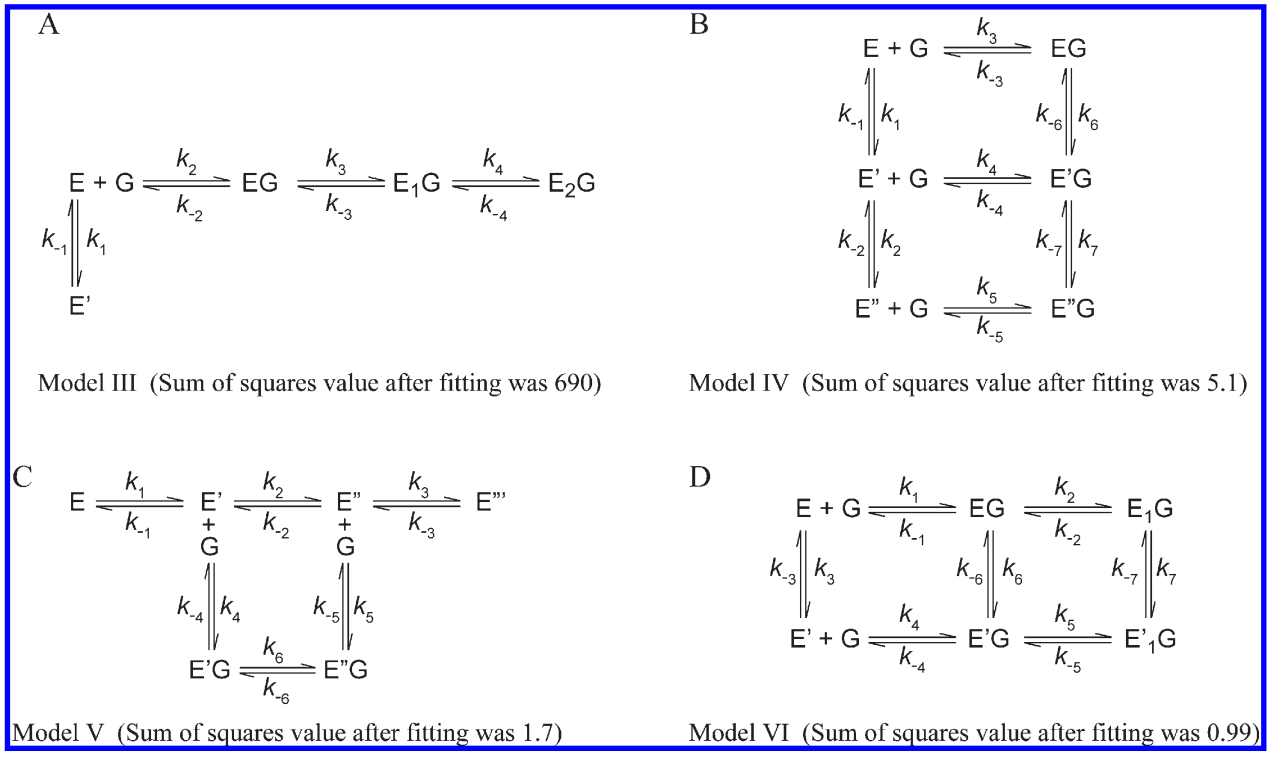

FIGURE 6: Experimental glucose binding curves were fit to different kinetic models (A−D) using numerical integration of the rate equations via global fit analysis. The best fit model, model VI, produces a sum of squares value of 0.98.

Table 3: Sensitivity of the Sum of Squares (SSQ) Values to Variations in the Microscopic Rate Constants around the Best Fit Value[a]

rate constant	best fit value of the rate constant	SSQ of the best fit	SSQ upon fixing the rate constant at 0.1k	SSQ upon fixing the rate constant at 10k
*k_1	1407 M^{-1} s^{-1}	0.98	24	3.6 (P)
*k_{-1}	1.1 s^{-1}	0.98	3.7 (P)	23
*k_2	0.04 s^{-1}	0.98	7.7 (P)	3.5 (P)
*k_{-2}	0.34 s^{-1}	0.98	4.9 (P)	14
k_3	0.015 s^{-1}	0.98	21	20
k_{-3}	0.009 s^{-1}	0.98	21	49
k_4	202 M^{-1} s^{-1}	0.98	65	240
k_{-4}	23 s^{-1}	0.98	220	78
k_5	2.9 s^{-1}	0.98	54	268
k_{-5}	0.2 s^{-1}	0.98	130	22
*k_6	0.012 s^{-1}	0.98	23	7.9 (P)
*k_{-6}	0.11 s^{-1}	0.98	2.2 (P)	55
*k_7	0.053 s^{-1}	0.98	11	2.7 (P)
*k_{-7}	0.003 s^{-1}	0.98	1.6 (P)	9.9

[a]Poorly constrained rate constants are denoted with an asterisk. Sum of squares values that are not significantly perturbed upon variation of the microscopic rate constants are indicated with a (P).

DISCUSSION

Four previous investigations of the transient-state kinetics of glucose binding to human glucokinase have been conducted (*23*, *31*−*33*). Surprisingly, the results of these studies failed to produce a consensus regarding the mechanism of glucokinase kinetic cooperativity. In each of the prior studies, low concentrations of enzyme were used. As a result, several low-amplitude fluorescence signals associated with glucose binding were difficult or impossible to detect. In this work, we employed high enzyme concentrations and long acquisition times to obtain the most complete description of glucose binding kinetics reported to date. We observed four kinetically distinguishable events at glucose concentrations ranging from 3 to 96 mM. At lower glucose concentrations, or at temperatures below 25 °C, one or more of these events became undetectable, as evidenced by the lower number of exponential terms required to fit binding curves collected under these conditions. Our results are consistent with the findings of Antoine et al. (*33*), who also detected four kinetically distinguishable events associated with glucose binding; however, in their studies, only the value of k_{obs3} was obtained with sufficient certainty to allow kinetic modeling. By comparison, our experiments afforded the acquisition of accurate rate constant and fluorescence amplitude data for all four observable events at a total of seven different glucose concentrations.

Viscosity and temperature variation studies provided insight into the nature of the events described by individual transient signals. The addition of the microviscogen glycerol produced a decrease in the magnitude of k_{obs1}, k_{obs2}, and k_{obs3}. The glycerol

dependencies of k_{obs1} and k_{obs3} were particularly strong for all glucose concentrations investigated. Because diffusional processes are expected to be most sensitive to solution viscosity, it seems reasonable to postulate that k_{obs1} and k_{obs3} describe, in part, the formation of the initial enzyme−glucose complex(es). Consistent with this speculation is the observation that both rate constants decrease in magnitude when the temperature is reduced from 25 to 10 °C. The value of k_{obs2} displays a more moderate response to increasing viscosity, making it more difficult to assign a specific physical process to this event. One possibility is that k_{obs2} describes a multitude of processes, one of which is associated with a diffusion-dependent event. Alternatively, k_{obs2} may reflect a conformational change that occurs after the initial association of the enzyme with glucose, the rate of which is only slightly affected by the presence of glycerol. The extent to which the rates of conformational change might be altered in the presence of added glycerol is unclear, although the response would likely depend upon both the nature and magnitude of the associated structural rearrangements. As previously observed by Neet and co-workers, we found that the slowest process associated with glucose binding, k_{obs4}, is largely independent of glycerol concentration (*23*). This fact, combined with the unique glucose dependence of k_{obs4}, complicates efforts to identify the process or processes that generate this signal. Control experiments conducted in this study exclude the possibility that k_{obs4} is caused by photobleaching.

Our ability to obtain accurate amplitude and rate constant data for each transient at a variety of glucose concentrations afforded the opportunity to apply global fit techniques to investigate the validity of specific kinetic models (*37*). We tested a number of potential mechanisms, including the glucose binding component of the mnemonic and LIST models. In each case, we attempted to fit our data to a minimal mechanism comprised of the smallest number of microscopic rate constants and the fewest enzyme species. A mechanism that included the presence of two unliganded species, E and E′, and four binary enzyme−glucose complexes produced a reasonable level of agreement with our experimental binding curves. It is worth noting that the various enzyme species present in our proposed model are capable of interconversion at all stages of the reaction coordinate. This model is similar to the initial LIST model put forth by Neet, except that it includes the formation of two intermediate enzyme−glucose complexes (EG and E′G) (*22*).

Although previous transient-state investigations have extracted microscopic rate constants based on a particular kinetic model, these approaches were often incomplete. Two studies failed to detect four kinetically distinguishable events associated with glucose binding (*31*, *32*), while a third neglected amplitude data associated with the transient-state binding curves (*33*). Our study represents the first attempt to globally fit glucose binding curves to a variety of kinetic models using the totality of rate constant and amplitude data obtained at a variety of glucose concentrations. The resulting values for the individual microscopic rate constants listed in Table 3 are derived from fitting 14 unknown variables, with limited constraints, to a kinetic model using transient-state binding data collected at seven different glucose concentrations. On the basis of this fact, caution should be used when considering the values of these microscopic rate constants (*38*). Indeed, we found that the values of several microscopic rate constants presented here are poorly constrained by our experimental data. Nevertheless, our results provide strong qualitative support for the kinetic pathway shown in Figure 6D. Further refinement of individual microscopic rate constant values awaits additional experimental investigation.

Human glucokinase is an attractive model for studying the role of conformational changes in enzyme action. The unique non-Michaelis−Menten kinetics observed in the steady-state velocity are intriguing because the enzyme functions exclusively as a monomer (*7*, *8*). On the basis of the transient-state glucose binding curves presented herein, we propose a minimal kinetic model in which the enzyme samples more than one conformationally distinct state, both in the absence and in the presence of glucose. The possibility that glucokinase continues to sample a rugged free energy landscape even after substrate association provides a wealth of opportunities for posttranslational regulation of the activity of this important metabolic enzyme.

ACKNOWLEDGMENT

We thank Professor Adrian Barbu for assistance with statistical analysis.

SUPPORTING INFORMATION AVAILABLE

Derivation of glucose dissociation constants, Tables S1 and S2, and Figures S1−S8. This material is available free of charge via the Internet at http://pubs.acs.org.

REFERENCES

1. Pilkis, J. S. (1968) Identification of human hepatic glucokinase and some properties of the enzyme. *Proc. Soc. Exp. Biol. Med. 129* (3), 681–684.
2. Matschinsky, F. M. (1990) Glucokinase as glucose sensor and metabolic signal generator in pancreatic β-cells and hepatocytes. *Diabetes 39*, 647–652.
3. Bell, G. I., and Polonsky, K. S. (2001) Diabetes mellitus and genetically programmed defects in β-cell function. *Nature 414*, 788–791.
4. Vionnet, N., Scoffel, M., Takeda, J., Yasuda, K., Bell, G. I., Zouali, H., Lesage, S., Velho, G., Iris, F., Passa, P., Froguel, P., and Cohen, D. (1992) Nonsense mutation in the glucokinase gene causes early-onset non-insulin dependent diabetes mellitus. *Nature 356*, 721–722.
5. Golyn, A. (2003) Glucokinase (GCK) mutations in hyper-and hypoglycemia: Maturity-onset diabetes of young, permanent neonatal diabetes and hyperinsulinemia of infancy. *Hum. Mutat. 22*, 353–362.
6. Holroyde, M. J., Allen, M. B., Storer, A. C., Warsy, A. S., Chesher, J. M. E., Trayer, J. P., Cornish-Bowden, A., and Walker, D. G. (1976) The purification in high yield and characterization of rat hepatic glucokinase. *Biochem. J. 153*, 163–373.
7. Storer, A., and Cornish-Bowden, A. (1976) Kinetics of rat liver glucokinase. Co-operative interactions with glucose at physiological significant concentrations. *Biochem. J. 159*, 7–14.
8. Cardenas, M. L., Rabajille, E., and Niemeyer, H. (1978) Maintenance of the monomeric structure of glucokinase under reacting conditions. *Arch. Biochem. Biophys. 190*, 142–148.
9. Moulay, A. M., and Van Schaftingen, E. (2001) Analysis of the cooperativity of human β-cell glucokinase through the stimulatory effect of glucose on fructose phosphorylation. *J. Biol. Chem. 276*, 3872–3878.
10. Gregoriou, M., Trayer, I. P., and Cornish-Bowden, A. (1981) Isotope-exchange evidence for an ordered mechanism for rat-liver glucokinase, a monomeric cooperative enzyme. *Biochemistry 20*, 499–506.
11. Pettersson, G. (1986) Mechanistic origin of the sigmoidal rate behaviour of glucokinase. *Biochem. J. 233*, 347–350.
12. Monasterio, O., and Cardenas, M. L. (2003) Kinetic studies of rat liver hexokinase D ('glucokinase') in non-cooperative conditions show an ordered mechanism with MgADP as the last product to be released. *Biochem. J. 371*, 29–38.
13. Richard, J., Meunier, J.-C., and Buc, J. (1974) Regulatory behavior of monomeric enzymes: The mnemonical enzyme concept. *Eur. J. Biochem. 49*, 195–208.
14. Ainslie, G. R., Jr., Shill, J. P., and Neet, K. E. (1972) Transients and cooperativity. A slow transition model for relating transients and cooperative kinetics of enzymes. *J. Biol. Chem. 247*, 7088–7096.
15. Ricard, J., Buc, J., and Meunier, J.-C. (1977) Enzyme memory. A transient kinetic study of wheat-germ hexokinase LI. *Eur. J. Biochem. 80*, 581–592.

16. Buc, J., Ricard, J., and Meunier, J.-C. (1977) Enzyme memory 2. Kinetics and thermodynamics of the slow conformation changes of wheat-germ hexokinase LI. *Eur. J. Biochem. 80*, 593–601.
17. Meunier, J.-C., Buc, J., and Ricard, J. (1979) Enzyme memory effect of glucose 6-phosphate and temperature on the molecular transition of wheat-germ hexokinase LI. *Eur. J. Biochem. 97*, 573–583.
18. Rabin, B. R. (1967) Co-operative effects in enzyme catalysis: A possible kinetic model based on substrate-induced conformation isomerization. *Biochem. J. 102* (2), 22C–23C.
19. Frieden, C. (1970) Kinetic aspects of regulation of metabolic processes. The hysteretic enzyme concept. *J. Biol. Chem. 245*, 5788–5799.
20. Neet, K. E. (1983) Cooperativity in enzyme function: Equilibrium and kinetic aspects. In Contemporary Enzyme Kinetics and Mechanism (Purich, D. L., Ed.) pp 267−320, Academic Press, New York.
21. Neet, K. E., and Ainslie, G. R., Jr. (1980) Hysteretic enzymes. *Methods Enzymol. 64*, 192–226.
22. Neet, K. E., Keenan, R. P., and Tippett, P. S. (1990) Observation of a kinetic slow transition in monomeric glucokinase. *Biochemistry 29*, 770–777.
23. Lin, S. X., and Neet, K. E. (1990) Demonstration of a slow conformational change in liver glucokinase by fluorescence spectroscopy. *J. Biol. Chem. 265* (17), 9670–9675.
24. Storer, A. C., and Cornish-Bowden, A. (1977) Kinetic evidence for a 'mnemonical' mechanism for rat liver glucokinase. *Biochem. J. 165* (1), 61–69.
25. Pollard-Knight, D., and Cornish-Bowden, A. (1987) Kinetics of hexokinase D ('glucokinase') with inositne triphosphate as phosphor-donor; loss of co-operativity with respect to glucose. *Biochem. J. 245*, 625–629.
26. Niemeyer, H., Cardenas, M. L., Rabajille, E., Ureta, T., Clark-Turri, L., and Pefnaranda, J. (1975) Sigmoidal kinetics of glucokinase. *Enzyme 20*, 321–333.
27. Cornish-Bowden, A., and Storer, A. C. (1986) Mechanistic origin of the sigmoidal rate behaviour of rat liver hexokinase D ('glucokinase'). *Biochem. J. 240*, 293–296.
28. Parry, M. J., and Walker, D. G. (1967) Further properties and possible mechanism of action of adenosine 5′-triphosphate-D-glucose 6-phosphotransferase from rat liver. *Biochem. J. 105* (2), 473–482.
29. Gonzalez, C., Ureta, T., Babul, J., Rabajille, E., and Niemeyer, H. (1967) Characterization of isoenzymes of adenosine triphosphate: D-Hexose 6-phosphotransferase from rat liver. *Biochemistry 6* (2), 460–468.
30. Kamata, K., Mitsuya, M., Nishimura, T., Eiki, J., and Nagata, Y. (2004) Structural basis for allosteric regulation of the monomeric allosteric enzyme human glucokinase. *Structure 12*, 429–438.
31. Heredia, V. V., Thomson, J., Nettleton, D., and Sun, S. (2006) Glucose-induced conformational changes in glucokinase mediate allosteric regulation: Transient kinetic analysis. *Biochemistry 45*, 7553–7562.
32. Kim, Y. B., Kalinowski, S. S., and Marcinkeviciene, J. (2007) A pre-steady state analysis of ligand binding to human glucokinase: Evidence for a preexisting equilibrium. *Biochemistry 46*, 1423–1431.
33. Antoine, M., Boutin, J. A., and Ferry, G. (2009) Binding kinetics of glucose and allosteric activators to human glucokinase reveal multiple conformational states. *Biochemistry 48*, 5466–5482.
34. Larion, M., and Miller, B. G. (2009) 23-Residue C-terminal α-helix governs kinetic cooperativity in monomeric human glucokinase. *Biochemistry 48*, 6157–6165.
35. Puxty, G., Maeder, M., Neuhold, Y. M., and King, P. (2005) Pro-Kineticist II, Applied Photophysics Ltd., Leatherhead, England.
36. Akaike, H. (1974) A new look at the statistical model identification. *IEEE Trans. Autom. Control 19*, 716–723.
37. Johnson, K. A., Simpson, Z. B., and Blom, T. (2009) Global Kinetic Explorer: A new computer program for dynamic simulation and fitting of kinetic data. *Anal. Biochem. 387*, 20–29.
38. Johnson, K. A., Simpson, Z. B., and Blom, T. (2009) FitSpace Explorer: An algorithm to evaluate multidimensional parameter space in fitting kinetic data. *Anal. Biochem. 387*, 30–41.